

pubs.acs.org/JPCC Article

Oxygen Reduction Electrocatalysis on Ordered Intermetallic Pd-Bi Electrodes Is Enhanced by a Low Coverage of Spectator Species

Yunfei Wang,[‡] Du Sun,[‡] Maoyu Wang, Zhenxing Feng, and Anthony Shoji Hall*



Cite This: J. Phys. Chem. C 2020, 124, 5220-5224



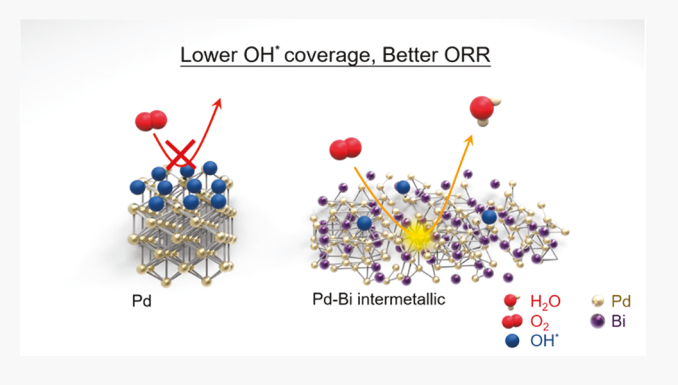
ACCESS

Metrics & More

Article Recommendations

3 Supporting Information

ABSTRACT: The sluggish rate of the oxygen reduction reaction (ORR) reduces the performance of fuel cell devices. We demonstrated that ordered intermetallic Pd_3Bi and $Pd_{31}Bi_{12}$ are up to $\sim 11 \times$ more active than state-of-the-art Pt/C and Pd/C catalysts for the ORR. Temperature-dependent electrochemical measurement indicates that the activation energy (E_a) for the ORR on $Pd_{31}Bi_{12}$ and Pd/C is lower than that of Pd_3Bi and Pt/C under a wide range of overpotentials. The resulting E_a indicates that a larger pre-exponential factor (surface site availability) is the primary reason for the enhanced ORR performance on Pd-Bi intermetallics. The increased number of active sites provides more available sites for O_2 activation and conversion, which agrees with the E_a measurements. This study deepens our understanding of catalyst-electrolyte and



catalyst—adsorbate interaction during the ORR on state-of-the-art Pd—Bi ordered intermetallic catalysts. Fundamental knowledge gained from this study suggests that further increasing the tolerance of the electrode active sites to the adsorption of spectator species by designing appropriate catalysts can improve the ORR performance.

■ INTRODUCTION

The oxygen reduction reaction (ORR) is an important half-reaction for renewable energy storage and conversion devices, such as fuel cells, and rechargeable metal—air batteries. However, the low activity and stability of the ORR catalyst causes a reduction in the performance of electrochemical devices, hindering their implementation for commodity energy storage and conversion. $^{18-20}$

Currently, Pt-group metals (PGM) are the most active materials for mediating the reduction of O2 to H2O. Overpotentials in excess of ~0.4 V are often required to drive the ORR at appreciable rates. Poisoning of the noble metal surface by spectator species, such as adsorbed hydroxyl or surface oxide, which reduce the amount of available active sites, is a major factor contributing to the large overpotentials required to drive the ORR at high rates.²¹ The removal of these species by reductive desorption is required for the ORR to proceed on metallic surface sites. However, the coverage of these species varies with potential, decreasing in coverage as the overpotential (η) for the ORR is increased. Complete removal of these spectator species often requires $\eta = \sim 0.4 - 0.5$ V. 21,23 Studies have indicated that the decreased coverage of spectator species is the primary reason for enhanced catalytic activity on some alloy systems, such as Pt-Ni disordered alloys, which is caused by a decreased binding strength of oxygen. 21,22 The decreased adsorption energy of oxygen on transition metal alloys arises from changes to the composition and structure of the crystal (electronic effects) and from the

local arrangement of active sites on the surface (geometric effects).

Recently, we reported high-performance ORR on metastable Pd₃₁Bi₁₂ ordered intermetallic materials by electrochemical deposition at room temperature.²⁴ Initial kinetic and surface analysis has indicated that the electron transfer barrier is reduced on Pd₃₁Bi₁₂ relative to Pd metal from a reduction in the O₂ adsorption energy as indicated by a downshift of the dband center.²⁴ We also reported high ORR activity on Pd₃Bi nanoparticles.²⁵ To the best of our knowledge, Pd₃Bi and Pd₃₁Bi₁₂ materials exhibit among the highest mass and specific ORR activities for Pd-based materials in alkaline electrolytes.^{24,25} We hypothesize that the increased activity of Pd₃₁Bi₁₂ and Pd₃Bi arises from a decrease in the population of spectator species at ORR-relevant potentials compared to elemental Pd.

Herein, we report that a decrease in the coverage of spectator species gives rise to greater surface site availability and therefore higher specific activity for the ORR on Pd-Bi ordered intermetallic compounds relative to Pd and Pt. To the best of our knowledge, this is the first report that experimentally validates that increases in surface site

Received: December 19, 2019 Revised: January 15, 2020 Published: February 3, 2020



availability enhance ORR catalysis on Pd-based ordered intermetallic systems.

METHODS

 $Pd_{31}Bi_{12}$ (R3 space group) and Pd_3Bi (Pmma space group) were prepared as described in our earlier articles. In brief, $Pd_{31}Bi_{12}$ was prepared from a solution of Na_2PdCl_4 and BiC_2H_3O , and a glassy carbon electrode was subjected to 200 cycles of potential pulses from -0.3~V vs NHE for 30 ms to 5 s at open circuit, followed by a constant voltage of -0.1~V vs NHE for 180 s. $^{26}~Pd_3Bi$ was prepared by electrochemical dealloying of $PdBi_2$ nanoparticles. $^{25}~The$ morphology and structural characterization of the Pd-Bi intermetallics can be found in our previous reports. 25,26

RESULTS

The ORR activity of Pd₃Bi and Pd₃₁Bi₁₂ was compared with commercial Pt/C (TKK, 40% Pt on high surface area carbon) and Pd/C (Premetek, 40% Pd on carbon) catalysts (Figure 1).

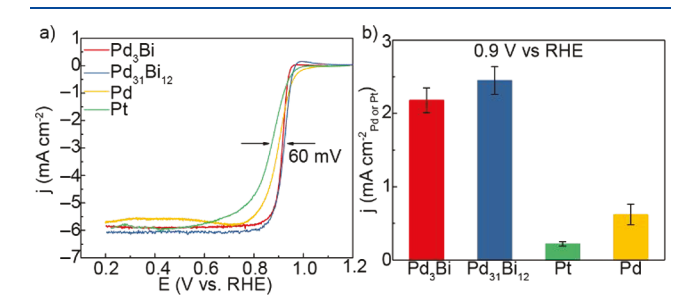


Figure 1. (a) LSVs and (b) specific activity at 0.9 V of Pt/C, Pd/C, Pd $_{31}$ Bi $_{12}$, and Pd $_{3}$ Bi in O $_{2}$ -saturated 0.1 M KOH. All voltammetry was collected on a 5 mm diameter glassy carbon rotating disk electrode (RDE) at 1600 rpm at a voltage sweep rate of 20 mV s $^{-1}$.

The onset potential of the ORR on both Pt/C and Pd/C was almost the same (\sim 1.02 V), which is in agreement with literature reports,²⁷ while the onset potentials for Pd₃Bi and Pd₃₁Bi₁₂ were more negative (~0.97 V). At more negative potentials (starting at ~0.95 V), we observed a rapid increase in the current for Pd₃Bi and Pd₃₁Bi₁₂, while the current for Pd/ C and Pt/C increased gradually. The half-wave potential of Pd₃Bi and Pd₃₁Bi₁₂ was more positive by 60 and 32 mV relative to Pt/C and Pd/C, respectively, indicating that it possesses superior catalytic activity relative to the commercial catalysts. The specific activity (SA) was measured by normalizing the kinetic current density to the ECSA of precious metal sites. 24,25 The SA of $Pd_{31}Bi_{12}$ was 2.42 ± 0.2 mA/cm $_{Pd}^2$ at 0.9 V vs RHE, and that of Pd₃Bi was 2.18 \pm 0.17 mA/cm²_{Pd}; both Pd-Bi alloys exhibit activities that are significantly higher than Pt/C $(0.22 \pm 0.03 \text{ mA/cm}_{Pt}^2)$ and Pd/C $(0.62 \pm 0.14 \text{ mA/cm}_{Pd}^2)$ at the same voltage (Figure 1b). The specific activity of Pd-Bi alloys is larger than that of elemental Pd or Pt, indicating that it exhibits superior catalytic activity.

To gain insight into the remarkable ORR performance of Pd–Bi alloys, we measured the effect of temperature (30–60 °C) on the electrode-kinetic profile to estimate the activation energy ($E_{\rm a}$) for the ORR (Figure 2). The ORR voltammogram shifted toward anodic (positive) potentials with increasing temperature, indicating an enhancement in ORR kinetics (Figure S1).^{28–30} The $E_{\rm a}$ was determined by constructing an Arrhenius plot (ln k vs 1/T plot) at fixed potential from the voltammetry data.

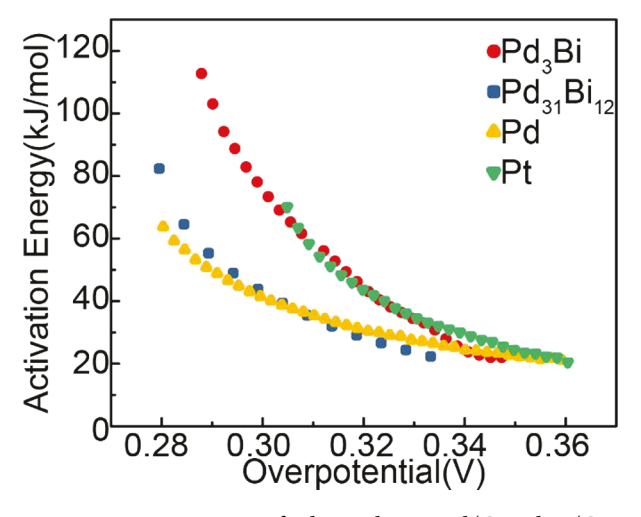


Figure 2. Activation energy of Pd_3Bi , $Pd_{31}Bi_{12}$, Pd/C, and Pt/C as a function of potential. All data was by measuring the mass-transport-corrected current densities at various voltages from 30 to 60 °C in 10 °C increments and fitting the data with the Arrhenius equation.

The apparent activation energy of all electrode materials monotonically decreases as the overpotential (η) is increased, saturating to \sim 20 kJ/mol for η > 0.34 V for all electrodes. The E_a of Pd₃Bi and Pt/C is comparable, and the E_a of Pd₃₁Bi₁₂ is comparable to that of Pd. The E_a of $Pd_{31}Bi_{12}$ and Pd is lower than that of Pd₃Bi and Pt/C for η < 0.34. However, Pd₃Bi and Pd₃₁Bi₁₂ both exhibit higher specific activity relative to Pd/C and Pt/C, despite having either a comparable or a larger E_a relative to Pd. To understand the significance of this, we need to consider the two factors which contribute to the overall performance of a catalyst (eq 1): (1) a lowering of the activation energy Ea, which is reflected as a decrease in the exponential portion of the Arrhenius equation, and (2) an increase in the pre-exponential factor, A (also known as the frequency factor), which represents the frequency of collisions between reactant molecules and the electrode. A lower activation barrier implies a larger per-site activity (turnover frequency), while an increase in the pre-exponential factor implies a larger fraction of sites is available to mediate catalysis. ^{21,31} Hence, both the pre-exponential factor and the E_a influence the observed catalytic rate constant.

$$k = Ae^{-E_a/RT} (1)$$

It is well known that oxide- or hydroxide-covered Pd/Pt sites are catalytically inactive toward the ORR, and these oxygenate species must be removed before the ORR can proceed. Hence, the catalytic rate is proportional to the fraction of nonpoisoned active sites available $(1 - \theta_{ads})$ and the turnover frequency (TOF) of each available site, as shown in eq 2.

rate
$$\propto (1 - \theta_{ads}) \times TOF$$
 (2)

The E_a is comparable to or higher than Pd/C across a wide range of potentials for Pd₃₁Bi₁₂ and Pd₃Bi, respectively. The enhanced activity of both Pd–Bi alloys relative to Pd/C was primarily caused by a larger pre-exponential factor in the Arrhenius equation (eq 1). The E_a is lower than or comparable to Pt/C across a wide range of potentials for Pd₃₁Bi₁₂ and Pd₃Bi, respectively. The enhanced activity of Pd–Bi alloys relative to Pt/C can be attributed to a larger pre-exponential factor for Pd₃Bi and to a combination of a larger pre-exponential factor and a higher intrinsic per-site activity for

 $Pd_{31}Bi_{12}$. Therefore, we can conclude that the higher specific activities for both Pd-Bi intermetallics relative to Pt/C and Pd/C is caused, primarily or in part, by a larger fraction of nonpoisoned Pd sites being available to mediate the ORR. The sluggish reduction kinetics of OH_{ads} spectator species on Pt/C and Pd/C is thought to reduce the fraction of active sites available, eroding its ORR performance. 23,34

To provide insight into the presence of spectator species, we measured surface redox events associated with oxygenate adsorption and desorption by cyclic voltammetry (Figure 3a).

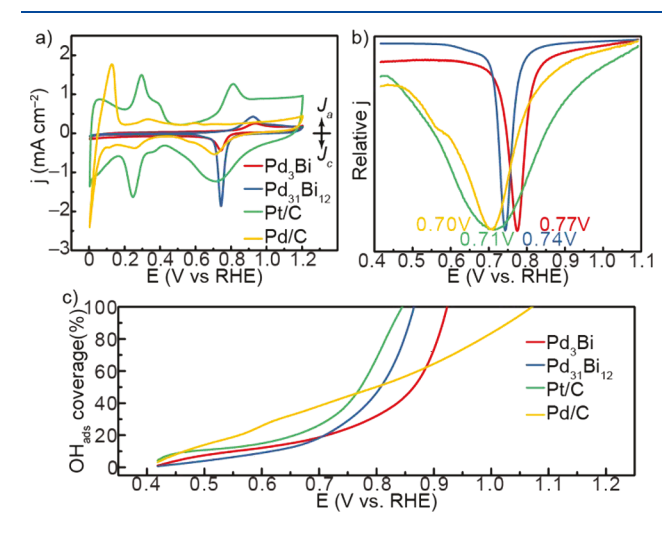


Figure 3. Cyclic voltammograms of Pd_3Bi , Pd/C, and Pt/C in (a) Arsaturated 0.1 M KOH. (b) Zoom in of the oxide-reduction features from a. (c) Surface coverage of OH_{ads} species calculated from the anodic branch of the CV from a. Sweep rate: 20 mV s⁻¹

The peak position for the reduction potential of electrochemically formed surface oxides is often used as a qualitative descriptor of the metal-oxygen (M-O) binding energy. 22,35, The peak potentials of Pt/Pd-O reduction of Pd₃₁Bi₁₂ and Pd₃Bi exhibit a cathodic shift relative to elemental Pd/C and Pt/C, indicating weaker binding energy of the M-O bond on Pd-Bi alloys (Figure 3b). The peak potential exhibits the trend Pd/C (0.71 V), Pt/C (0.71 V) < Pd₃₁Bi₁₂ (0.74 V) <Pd₃Bi (0.75 V) in order of decreased M-O binding energy. In addition, the width of the reduction peaks of the Pd-Bi alloys is significantly narrower than that of Pd/C and Pt/C, indicating that the adsorption energy of oxygen species depends weakly on coverage.³⁷ This is in stark contrast to elemental Pt and Pd nanoparticles which have broad oxidation and reduction features which arise from repulsive interactions between adsorbates as the surface coverage increases.³⁷

To assess the degree of oxygenate poisoning, the potential-dependent surface oxygenate coverage was measured by determining the charge passed during an anodic LSV and normalizing to the ECSA and charge associated with OH adsorption (OH_{ads}) or surface oxide (Figure 3a). We observe an anodic wave centered at $\sim\!0.93$ V for both Pd₃Bi and Pd₃₁Bi₁₂, followed by broad anodic features for more positive voltages. We ascribe this feature to OH_{ads} or surface oxidation of Pd/C. In contrast, Pd exhibits small anodic waves at $\sim\!0.6$ V, followed by a broad anodic current as the voltage is increased, while Pt/C exhibits an oxidative wave centered at $\sim\!0.8$ V followed by broad anodic current as the voltage is increased. We ascribe the anodic features that appeared at voltages < 0.9 V to arise from OH_{ads} formation on Pd/C and Pt/C. 38

However, the speciation of oxygenate species as a function of potential on Pd-Bi alloys is not known; hence, it is possible that surface oxidation rather than OH_{ads} adsorption may occur. Surface oxide formation was not observed to occur for $E \leq$ 0.93 V since we did not observe any change in the Pd K-edge white line intensity measured by in situ X-ray adsorption nearedge spectroscopy (XANES) on Pd-Bi alloys and Pd metal (Figure S2); henceforth, the spectator species will be assumed to be OH_{ads} . The formation of OH_{ads} was observed on the surface of Pd-Bi intermetallics at voltages more positive than 0.7 V, while on Pt and Pd, OHads formation monotonically increases at voltages more positive than 0.6 and 0.55 V, respectively (Figure 3c).⁴² Coverages of OH_{ads} over 100% would indicate the formation of surface oxide species or oxyhydroxide species, hence we truncated the data in Figure 3C at 100% coverage to reflect only OH_{ads} species. The ORR voltammograms reached diffusion-limited current densities at ~0.6 V for Pt and Pd and at ~0.8 V for the Pd-Bi alloys, which is near the onset of surface oxygenate formation on Pd/ C, Pt/C, and Pd-Bi intermetallics (Figure 3a).

To provide further confirmation that the surface oxygenate coverage is lower on Pd–Bi than on Pt or Pd we performed bulk CO electro-oxidation, since the rate of this reaction is determined by both the surface coverages of CO_{ads} and OH_{ads} and the probability of interaction of these two adsorbed species (eq 3).⁴³

$$CO_{ads} + OH_{ads} + OH^{-} \rightarrow CO_{2} + e^{-} + H_{2}O$$
 (3)

The adsorption of OH_{ads} has been measured on defect/step sites of Pt single crystals in 0.1 M KOH electrolytes at voltages as low as $\sim 0.1-0.2$ V, and it has been experimentally shown that underpotentially deposited hydrogen (H-UPD) and OH can place exchange. Therefore, CO oxidation can occur when the surface has a minority population of electrosorbed OH_{ads}, suggesting that this method can be more sensitive for probing the $\mathrm{OH}_{\mathrm{ads}}$ surface population than inert gas voltammograms. 38,43 In addition, this method is sensitive only to OH_{ads}, as surface oxide formation will decrease the fraction of sites available for CO oxidation. The electrooxidation of bulk CO onsets at 0.3 V for Pt, 0.4 V for Pd, although the increase in current after these voltages are modest, indicating that there is a small population of OH_{ads} is in the H-UPD region, in the so-called pre-ignition region (Figure 4).²⁹ There is no observation of a pre-ignition region on Pd-Bi alloys, indicating that the population of OH_{ads} is nearly null for voltages $< \sim 0.6$ V. At voltages more positive than 0.45 V for Pt, 0.55 V for Pd, and ~0.63 V for both Pd-Bi alloys, the CO electro-oxidation current rapidly increases, indicating that the population of OH_{ads} was increasing rapidly. At more positive voltages, the CO electro-oxidation rate decreased as the surface became covered by a surface oxide. The differences in CO electro-oxidation activity between Pd/C and Pt/C, in comparison with the OH_{ads} coverages estimated by the inert gas LSVs, may be due to differences in OH_{ads} and CO_{ads} mobility on these surfaces, which will alter the probability of collisions between these adsorbates. Taken together, the LSVs collected Ar- and CO-saturated solutions indicate that the surface population of the OHads spectator species is lower on Pd-Bi intermetallics than that on Pt/C and Pd/C at ORR-relevant potentials, giving rise to superior catalytic activity for the ORR.

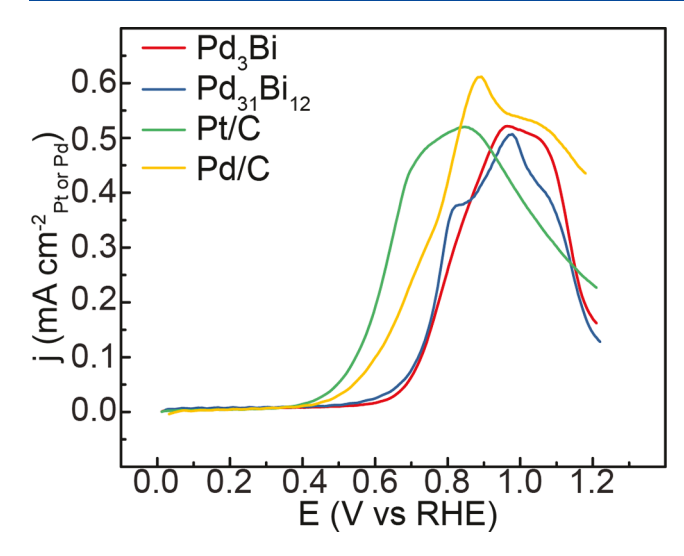


Figure 4. Linear sweep voltammograms of converted $Pd_{31}Bi_{12}$, Pd_3Bi , Pd/C, and Pt/C in CO-saturated 0.1 M KOH. LSVs in both panels are normalized to the ECSA of the electrode. Sweep rate: 20 mV s⁻¹.

CONCLUSION

In summary, we demonstrated that the origin of the high catalytic activity for the ORR on Pd–Bi ordered intermetallics primarily arises from the decreased adsorption energy of oxygen, which leads to lower coverage of spectator $\mathrm{OH}_{\mathrm{ads}}$, permitting more surface sites to be available for mediating O_2 conversion. This paper deepens our understanding catalyst–electrolyte and catalyst–adsorbate interactions during the ORR on our newly designed Pd–Bi ordered intermetallic catalysts. Fundamental knowledge gained from this study suggests that further increasing the tolerance of electrode active sites to the adsorption of oxygenate spectator species can enhance the ORR performance.

ASSOCIATED CONTENT

Supporting Information

The Supporting Information is available free of charge at https://pubs.acs.org/doi/10.1021/acs.jpcc.9b11734.

Temperature-dependent oxygen reduction electrocatalysis; materials; methods; synthesis of Pd-Bi nanoparticles; synthesis of Pd $_{31}$ Bi $_{12}$ nanoparticles; physicochemical characterization; oxygen reduction measurements; CO-stripping measurements; sample preparation for ICP-MS analysis; in-situ X-ray absorption spectroscopy measurements; temperature-dependent experiment; Koutechy-Levich kinetics and determination of n values; activation energy determination (PDF)

AUTHOR INFORMATION

Corresponding Author

Anthony Shoji Hall — Department of Materials Science and Engineering and Department of Chemistry, Johns Hopkins University, Baltimore, Maryland 21218, United States;

orcid.org/0000-0003-4134-4160; Email: shoji@jhu.edu

Authors

Yunfei Wang — Department of Materials Science and Engineering, Johns Hopkins University, Baltimore, Maryland 21218, United States Du Sun – Department of Materials Science and Engineering, Johns Hopkins University, Baltimore, Maryland 21218, United States

Maoyu Wang — School of Chemical, Biological, and Environmental Engineering, Oregon State University, Corvallis, Oregon 97331, United States

Zhenxing Feng — School of Chemical, Biological, and Environmental Engineering, Oregon State University, Corvallis, Oregon 97331, United States; orcid.org/0000-0001-7598-5076

Complete contact information is available at: https://pubs.acs.org/10.1021/acs.jpcc.9b11734

Author Contributions

‡Y.W. and D.S.: Cofirst authors.

Notes

The authors declare no competing financial interest.

ACKNOWLEDGMENTS

A.S.H. acknowledges financial support from the National Science Foundation under award no. CHE-1764310 and a Johns Hopkins University Catalyst Award. Z.F. thanks the startup financial support from Oregon State University. X-ray absorption spectroscopy measurements were done at the Stanford Synchrotron Radiation Lightsource (SSRL) experimental section 2-2. Use of SSRL, a SLAC National Accelerator Laboratory, was supported by the U.S. Department of Energy, Office of Science, Office of Basic Energy Sciences under Contract No. DE-AC02-76SF00515.

REFERENCES

- (1) Steele, B. C. H.; Heinzel, A. Materials for fuel-cell technologies. *Nature* **2001**, *414*, 345–352.
- (2) Wang, Z. L.; Xu, D.; Xu, J. J.; Zhang, X. B. Oxygen electrocatalysts in metal-air batteries: From aqueous to nonaqueous electrolytes. *Chem. Soc. Rev.* **2014**, *43*, 7746–7786.
- (3) Park, S.; Shao, Y.; Liu, J.; Wang, Y. Oxygen electrocatalysts for water electrolyzers and reversible fuel cells: Status and perspective. *Energy Environ. Sci.* **2012**, *5*, 9331–9344.
- (4) Bu, L.; Ding, J.; Guo, S.; Zhang, X.; Su, D.; Zhu, X.; Yao, J.; Guo, J.; Lu, G.; Huang, X. A general method for multimetallic platinum alloy nanowires as highly active and stable oxygen reduction catalysts. *Adv. Mater.* **2015**, *27*, 7204–7212.
- (5) Bu, L.; Guo, S.; Zhang, X.; Shen, X.; Su, D.; Lu, G.; Zhu, X.; Yao, J.; Guo, J.; Huang, X. Surface engineering of hierarchical platinum-cobalt nanowires for efficient electrocatalysis. *Nat. Commun.* **2016**, *7*, 11850.
- (6) Bu, L.; Shao, Q.; Pi, Y.; Yao, J.; Luo, M.; Lang, J.; Hwang, S.; Xin, H.; Huang, B.; Guo, J.; et al. Coupled s-p-d exchange in facet-controlled Pd3Pb tripods enhances oxygen reduction catalysis. *Chem.* **2018**, *4*, 359–371.
- (7) Kim, C.; Dionigi, F.; Beermann, V.; Wang, X.; Möller, T.; Strasser, P. Alloy nanocatalysts for the electrochemical oxygen reduction (ORR) and the direct electrochemical carbon dioxide reduction reaction (CO2RR). *Adv. Mater.* **2019**, *31*, 1805617.
- (8) Xiong, Y.; Yang, Y.; Joress, H.; Padgett, E.; Gupta, U.; Yarlagadda, V.; Agyeman-Budu, D. N.; Huang, X.; Moylan, T. E.; Zeng, R.; et al. Revealing the atomic ordering of binary intermetallics using in situ heating techniques at multilength scales. *Proc. Natl. Acad. Sci. U. S. A.* **2019**, *116*, 1974–1983.
- (9) Yang, Y.; Xiao, W.; Feng, X.; Xiong, Y.; Gong, M.; Shen, T.; Lu, Y.; Abruña, H. D.; Wang, D. Golden palladium zinc ordered intermetallics as oxygen reduction electrocatalysts. *ACS Nano* **2019**, 13, 5968–5974.

- (10) Carmo, M.; Doubek, G.; Sekol, R. C.; Linardi, M.; Taylor, A. D. Development and electrochemical studies of membrane electrode assemblies for polymer electrolyte alkaline fuel cells using faa membrane and ionomer. *J. Power Sources* **2013**, 230, 169–175.
- (11) Liu, J.; Talarposhti, M. R.; Asset, T.; Sabarirajan, D. C.; Parkinson, D. Y.; Atanassov, P.; Zenyuk, I. V. Understanding the role of interfaces for water management in platinum group metal-free electrodes in polymer electrolyte fuel cells. *ACS Appl. Energy Mater.* **2019**, *2*, 3542–3553.
- (12) Ko, J. S.; Parker, J. F.; Vila, M. N.; Wolak, M. A.; Sassin, M. B.; Rolison, D. R.; Long, J. W. Electrocatalyzed oxygen reduction at manganese oxide nanoarchitectures: From electroanalytical characterization to device-relevant performance in composite electrodes. *J. Electrochem. Soc.* 2018, 165, H777—H783.
- (13) Huang, X.; Shen, T.; Zhang, T.; Qiu, H.; Gu, X.; Ali, Z.; Hou, Y. Efficient oxygen reduction catalysts of porous carbon nanostructures decorated with transition metal species. *Adv. Energy Mater.* **2019**, 1900375.
- (14) Wang, H.-F.; Tang, C.; Zhang, Q. A review of precious-metal-free bifunctional oxygen electrocatalysts: Rational design and applications in Zn—air batteries. *Adv. Funct. Mater.* **2018**, 28, 1803329.
- (15) Luo, M.; Zhao, Z.; Zhang, Y.; Sun, Y.; Xing, Y.; Lv, F.; Yang, Y.; Zhang, X.; Hwang, S.; Qin, Y.; et al. PdMo bimetallene for oxygen reduction catalysis. *Nature* **2019**, *574*, 81–85.
- (16) Zhang, C.; Zhang, W.; Yu, S.; Wang, D.; Zhang, W.; Zheng, W.; Wen, M.; Tian, H.; Huang, K.; Feng, S.; et al. Unlocking the electrocatalytic activity of chemically inert amorphous carbon-nitrogen for oxygen reduction: Discerning and refactoring chaotic bonds. *ChemElectroChem* **2017**, *4*, 1269–1273.
- (17) Zhang, C.; Yu, S.; Xie, Y.; Zhang, W.; Zheng, K.; Drewett, N. E.; Yoo, S. J.; Wang, Z.; Shao, L.; Tian, H.; et al. Suppressing the pd-c interaction through b-doping for highly efficient oxygen reduction. *Carbon* **2019**, *149*, 370–379.
- (18) Nørskov, J. K.; Rossmeisl, J.; Logadottir, A.; Lindqvist, L.; Kitchin, J. R.; Bligaard, T.; Jónsson, H. Origin of the overpotential for oxygen reduction at a fuel-cell cathode. *J. Phys. Chem. B* **2004**, *108*, 17886–17892.
- (19) Esposito, D. V.; Chen, J. G. Monolayer platinum supported on tungsten carbides as low-cost electrocatalysts: Opportunities and limitations. *Energy Environ. Sci.* **2011**, *4*, 3900–3912.
- (20) Raciti, D.; Kubal, J.; Ma, C.; Barclay, M.; Gonzalez, M.; Chi, M.; Greeley, J.; More, K. L.; Wang, C. Pt3re alloy nanoparticles as electrocatalysts for the oxygen reduction reaction. *Nano Energy* **2016**, 20, 202–211.
- (21) Stamenkovic, V. R.; Fowler, B.; Mun, B. S.; Wang, G.; Ross, P. N.; Lucas, C. A.; Marković, N. M. Improved oxygen reduction activity on Pt3Ni(111) via increased surface site availability. *Science* **2007**, 315, 493–497.
- (22) Huang, X.; Shumski, A. J.; Zhang, X.; Li, C. W. Systematic control of redox properties and oxygen reduction reactivity through colloidal ligand-exchange deposition of pd on au. *J. Am. Chem. Soc.* **2018**, *140*, 8918–8923.
- (23) Jia, Q.; Caldwell, K.; Ziegelbauer, J. M.; Kongkanand, A.; Wagner, F. T.; Mukerjee, S.; Ramaker, D. E. The role of OOH binding site and pt surface structure on ORR activities. *J. Electrochem. Soc.* **2014**, *161*, F1323–F1329.
- (24) Wang, Y.; Sun, D.; Chowdhury, T.; Wagner, J. S.; Kempa, T. J.; Hall, A. S. Rapid room-temperature synthesis of a metastable ordered intermetallic electrocatalyst. *J. Am. Chem. Soc.* **2019**, *141*, 2342–2347.
- (25) Sun, D.; Wang, Y.; Livi, K. J. T.; Wang, C.; Luo, R.; Zhang, Z.; Alghamdi, H.; Li, C.; An, F.; Gaskey, B.; et al. Ordered intermetallic Pd3 Bi prepared by an electrochemically induced phase transformation for oxygen reduction electrocatalysis. *ACS Nano* **2019**, *13*, 10818–10825.
- (26) Wang, Y.; Hall, A. S. Pulsed electrodeposition of metastable Pd31Bi12 nanoparticles for oxygen reduction electrocatalysis. *ACS Energy Lett.* **2020**, *5*, 17–22.

- (27) Jiang, L.; Hsu, A.; Chu, D.; Chen, R. Oxygen reduction reaction on carbon supported Pt and Pd in alkaline solutions. *J. Electrochem. Soc.* **2009**, *156*, B370–B376.
- (28) Paulus, U. A.; Schmidt, T. J.; Gasteiger, H. A.; Behm, R. J. Oxygen reduction on a high-surface area Pt/Vulcan carbon catalyst: A thin-film rotating ring-disk electrode study. *J. Electroanal. Chem.* **2001**, 495, 134–145.
- (29) Schmidt, T. J.; Stamenkovic, V.; Ross, P. N., Jr.; Markovic, N. M. Temperature dependent surface electrochemistry on pt single crystals in alkaline electrolyte part 3. The oxygen reduction reaction. *Phys. Chem. Phys.* **2003**, *S*, 400–406.
- (30) Wakabayashi, N.; Takeichi, M.; Itagaki, M.; Uchida, H.; Watanabe, M. Temperature-dependence of oxygen reduction activity at a platinum electrode in an acidic electrolyte solution investigated with a channel flow double electrode. *J. Electroanal. Chem.* **2005**, *574*, 339–346.
- (31) Anderson, A. B.; Roques, J.; Mukerjee, S.; Murthi, V. S.; Markovic, N. M.; Stamenkovic, V. Activation energies for oxygen reduction on platinum alloys: Theory and experiment. *J. Phys. Chem. B* **2005**, *109*, 1198–1203.
- (32) Ramaswamy, N.; Mukerjee, S. Fundamental mechanistic understanding of electrocatalysis of oxygen reduction on Pt and non-Pt surfaces: Acid versus alkaline media. *Adv. Phys. Chem.* **2012**, 2012. 1.
- (33) Shinagawa, T.; Garcia-Esparza, A. T.; Takanabe, K. Insight on tafel slopes from a microkinetic analysis of aqueous electrocatalysis for energy conversion. *Sci. Rep.* **2015**, *5*, 13801.
- (34) Teliska, M.; Murthi, V. S.; Mukerjee, S.; Ramaker, D. E. Correlation of water activation, surface properties, and oxygen reduction reactivity of supported Pt–M/C bimetallic electrocatalysts using xas. *J. Electrochem. Soc.* **2005**, *152*, A2159–A2169.
- (35) Hu, J. W.; Li, J. F.; Ren, B.; Wu, D.-Y.; Sun, S. G.; Tian, Z. Q. Palladium-coated gold nanoparticles with a controlled shell thickness used as surface-enhanced raman scattering substrate. *J. Phys. Chem. C* **2007**, *111*, 1105–1112.
- (36) Naohara, H.; Ye, S.; Uosaki, K. Thickness dependent electrochemical reactivity of epitaxially electrodeposited palladium thin layers on Au(111) and Au(100) surfaces. *J. Electroanal. Chem.* **2001**, *500*, 435–445.
- (37) McCrum, I. T.; Janik, M. J. First principles simulations of cyclic voltammograms on stepped Pt(553) and Pt(533) electrode surfaces. *ChemElectroChem* **2016**, *3*, 1609–1617.
- (38) Wang, J. X.; Markovic, N. M.; Adzic, R. R. Kinetic analysis of oxygen reduction on Pt(111) in acid solutions: Intrinsic kinetic parameters and anion adsorption effects. *J. Phys. Chem. B* **2004**, *108*, 4127–4133.
- (39) Wang, M.; Árnadóttir, L.; Xu, Z. J.; Feng, Z. In situ X-ray absorption spectroscopy studies of nanoscale electrocatalysts. *Nano-Micro Lett.* **2019**, *11*, 47.
- (40) Liao, H.; Wei, C.; Wang, J.; Fisher, A.; Sritharan, T.; Feng, Z.; Xu, Z. J. A multisite strategy for enhancing the hydrogen evolution reaction on a nano-Pd surface in alkaline media. *Adv. Energy Mater.* **2017**, *7*, 1701129.
- (41) Ravel, B.; Newville, M. Athena, artemis, hephaestus: Data analysis for X-ray absorption spectroscopy using ifeffit. *J. Synchrotron Radiat.* **2005**, *12*, 537–541.
- (42) Peuckert, M. XPS investigation of surface oxidation layers on a platinum electrode in alkaline solution. *Electrochim. Acta* **1984**, 29 (10), 1315–1320.
- (43) Blizanac, B. B.; Lucas, C. A.; Gallagher, M. E.; Arenz, M.; Ross, P. N.; Marković, N. M. Anion adsorption, co oxidation, and oxygen reduction reaction on a Au(100) surface: The ph effect. *J. Phys. Chem. B* **2004**, *108*, 625–634.